Hyperspectral image super-resolution algorithm via sparse representation based on spectral similarity

Liu Yongfeng[1,2], Wang Nian[1,3*], Wang Feng[2], Li Congli[2], Liu Xiao[2], Xu Guoming[4]

(1. School of Electronics and Information Engineering, Anhui University, Hefei 230601, China; 2. Army Artillery and Air Defense Forces College & Key Laboratory of Polarization Imaging Detection Technology in Anhui Province, Hefei 230031, China; 3. Key Laboratory of Intelligent Computing and Signal Processing of the Ministry of Education, Anhui University, Hefei 230039, China; 4. Information Engineering College, Anhui Xinhua University, Heifei 230009, China)

Abstract: Hyperspectral image sparse super-resolution algorithm based on spectral similarity was proposed to improve low spatial resolution of hyperspectral images. The super resolution algorithm, based on the criterion of maximum likelihood estimation and Gaussian mixture sparse representation, assigned various weights to different coding residuals to improve spatial resolution of reconstructed images and the robustness to noise. Based on spectral similarity, the super-resolution model which added sparsity constraints using pixel spectral similarity was proposed to ensure the accuracy of the spectrum images. The experiments have been run to prove that this model achieves a better result than Bicubic, Yang and Pan algorithms in both visual effect and objective measures. Additionally, various parameters in the reconstruction were analyzed in order to provide better image detection and classification.

Key words: hyperspectral image; sparse representation; spectral similarity; super-resolution

CLC number: TP751 **Document code:** A **DOI:** 10.3788/IRLA201948.S128003

基于谱间相似性的高光谱图像稀疏超分辨率算法

刘永峰[1,2],王 年[1,3*],王 峰[2],李从利[2],刘 晓[2],徐国明[4]

(1. 安徽大学 电子信息工程学院,安徽 合肥 230601;2. 陆军炮兵防空兵学院 偏振光成像探测技术安徽省重点实验室,安徽 合肥 230031;3. 安徽大学 计算智能与信号处理教育部重点实验室,安徽 合肥 230039;4. 安徽新华学院 信息工程学院, 安徽 合肥 230009)

摘 要: 为解决高光谱图像空间分辨率较低的问题, 文中提出了一种基于谱间相似性的高光谱图像稀疏超分辨率算法。该算法在最大似然估计准则下,构建了基于混合高斯的稀疏超分辨率编码模型,针对不同的分解残差自适应分配权重,提高了重建图像的空间分辨率和算法对噪声的鲁棒性;该算法构建了基于谱间相似性的图像超分辨率模型, 将高光谱图像中普遍存在的像元光谱相关性作为稀疏约束项,保证了图像重建时光谱信息的准确性。实验表明,与 Bicubic、Yang、Pan 算法相比,文中算法在主观视觉效果、客观评价指标等方面均具有一定优势,验证了算法的有效性。最后将算法各项参数对重建效果的影响进行了分析,为图像检测、分类等应用提供了有效前提。

关键词: 高光谱图像; 稀疏表示; 谱间相似性; 超分辨率

收稿日期: 2018-11-10; **修订日期:** 2018-12-20

基金项目: 国家自然科学基金(41406109);中国博士后科学基金(2016M592961);安徽省自然科学基金(1608085MF140, 1708085QD90)

作者简介: 刘永峰(1981-),男,讲师,博士生,主要从事高光谱成像与处理方面的研究。Email: 954271756@qq.com

通讯作者: 王年(1966-),男,教授,博士生导师,主要从事计算视觉、模式识别和生物信号处理方面的研究。Email: wn_xlb@abu.edu.cn

0 Introduction

With rapid development of modern science and technology, hyperspectral remote sensing science, as a comprehensive high-tech, has been widely and profoundly advanced in theory, technology and application[1]. It is a multi-dimension information acquisition technology that combines target detection technology and spectral imaging technology. It can simultaneously acquire two-dimensional spatial information describing the distribution of ground features and one-dimensional spectral information describing the spectral characteristics of the ground features. The spectral range covering visible light, near-infrared, short-wave infrared and mid-infrared bands have spectral resolutions on the order of nanometers, making many spectral information that could not be acquired in multispectral remote sensing images be detected[2].

Although hyperspectral image has very high spectral resolution, with increasing spectral bands in the images, the physical size of the sensitization element needs to be increased to maintain image quality[3]. High spatial resolution images are in high demand in many areas including target recognition, object classification and environmental change detection. Due to the limitation of hardware, the focus of the research has been shifted to software development to improve spatial resolution of hyperspectral images.

Image super-resolution (SR) refers to reconstruction of high resolution (HR) images by one or more low resolution (LR) images through information processing [4-5]. The concept of restoration was first proposed by J. L. Harris[6] and J. W. Goodman[7] in 1964 and 1968. The method is named after Harris and Goodman as Harris-Goodman spectral extrapolation method. Many researchers subsequently proposed various restoration methods. There are three main types of hyperspectral image super-resolution methods: interpolation[8], reconstruction[9] and learning[10]. The interpolation method is the simplest method to achieve hyperspectral image super-resolution, but the effect can not meet the desired requirements, such as bilinear interpolation, bicubic interpolation and so on. The reconstruction method uses mathematical modeling to mine the effective prior information of hyperspectral images, and relies on the redundant complementary information between multiple images. The computational cost of the algorithm is high, such as IBP, POCS and so on. The learning method can obtain better results, but the training samples are more demanding, the training cycle is longer, and the parameters are difficult to adjust, such as PCA, wavelet, sparse and so on. During the past few years, hyperspectral image super-resolution restoration method, based on sparse representation model, has managed to gain more interest globally. Zhao et al.[11] proposed a hyperspectral image super-resolution algorithm supported by pixel decomposition, using the end-member abundance in the pixel to construct a spectral constraint term to ensure accuracy of the reconstructed image spectrum. This method has higher requirements on image end-member extraction and pixel decomposition accuracy during the reconstruction process. Huang et al. fused low-spatial-resolution hyperspectral images and high-resolution images by non-parametric Bayesian sparse representation, and combined the spatial structure information of images with the spectral domain information of hyperspectral images to avoid the spectral distortion of reconstructed images. This method has its own limitation in terms of obtaining images in the same region. Pan et al.[12] used the structural self-similarity between images and the spectral similarity of the pixels to enhance the spatial resolution of the image, and reduced the spectral dimension by principal component analysis to improve the computational efficiency. Fu et al.[13] combined with matrix decomposition and image fusion, and used sparse representation theory, total variation, non-local self-similarity and correlation

optimization methods to achieve high-resolution spectral image reconstruction, improve the accuracy of non-negative sparse coding and the visual effect of reconstruction.

The above hyperspectral image super-resolution algorithm based on sparse representation has two problems. Firstly, accuracy of the algorithm relies on information other than the hyperspectral image or other algorithms, such as [11]. Secondly, it′s poor robustness in reconstruction using image spectrum information, such as [12] and [13]. In this paper, we proposed a hyperspectral image super-resolution algorithm via sparse representation based on spectral similarity to solve those problems. Hyperspectral image sparse super-resolution algorithm is proposed by this paper to improve low spatial resolution of hyperspectral images based on spectral similarity. The super resolution algorithm, based on the criterion of maximum likelihood estimation and Gaussian mixture sparse representation, assigned various weights to different coding residuals to improve spatial resolution of reconstructed images which can be generalized to various test sets. Moreover, the correlation of the spectral information of the pixels present in the hyperspectral image is used as a sparse constraint condition in the image reconstruction to improve the spectral accuracy of the pixel of the algorithm. Compared to the method of interpolation and Yang et al, effectiveness of this algorithm has been verified. In addition, the influence of the different parameters on the image reconstruction will be discussed in the following paragraphs.

1 Related work

1.1 Super-resolution model based on sparse representation

The basic idea of sparse coding is to assume that the natural signal can be represented by compression or by a predefined linear combination of atoms. Let the signal be $x \in R^N$, its sparse representation be expressed as[14]:

$$\min\|\alpha\|_p \quad \text{s.t. } \|x-D\alpha\|_2^2 \leqslant \varepsilon \tag{1}$$

Wherein α is a sparse representation coefficient of x, $D \in R^{N\times M}$ $(M>N)$ is a over-complete dictionary, each column vector is called an atom which is recorded as d_i $(i=1,2, \cdots M)$, $\|\cdot\|_p$ is the L_p norm, and ε is an approximation error value.

Generally, the degenerate model of the image can be expressed as:

$$Y=SHX+v \tag{2}$$

Where $X \in R^N$ denotes the original high resolution image, $Y \in R^M$ denotes the low resolution image, $S \in R^{N\times M}$ shows the down sampling matrix, $H \in R^{N\times M}$ denotes the fuzzy matrix, and $v \in R^M$ denotes the additive random noise.

Assuming D_h is a high resolution dictionary, then it can be learned from high resolution image samples, so the ideal image X can be linearly represented by its sparse representation coefficient α:

$$X=D_h\alpha \tag{3}$$

Then, the problem of super-resolution reconstruction is transformed from a low resolution image to its sparse representation coefficient:

$$Y=SHX=SHD_h\alpha \tag{4}$$

And the low resolution dictionary D_l can be obtained by D_h through the down sampling, so high resolution reconstruction image $X=D_h\alpha$ can be obtained via:

$$\min_{\alpha}\|\alpha\|_0 \quad \text{s.t. } \|D_l\alpha-Y\|_2^2 \leqslant \varepsilon \tag{5}$$

1.2 Sparse coding Gaussian mixture model

D is represented by $D=[p_1, p_2, \cdots, p_n]^{\mathrm{T}}$, where the vector p_i is i th line of D, and let $e=Y-D\alpha=[e_1, e_2, \cdots, e_n]^{\mathrm{T}}$ is the decomposition residual, so $e_i=y_i-p_i\alpha$. According to the difference of e of prior knowledge, the form of the solution that conforms to the maximum likelihood estimation criterion is different. If e obeys Laplasse distribution, we only use L_1 norm $\|Y-D\alpha\|_1 \leqslant \varepsilon$ to determine the error of e,

which is consistent with the maximum likelihood estimation rule. If e obeys Gauss distribution, then L_2 norm $\|Y-D\alpha\|_2^2 \leqslant \varepsilon$ can meet the maximum likelihood estimation rule. But in fact, e is neither obeying Laplasse distribution nor obeying Gauss distribution. Therefore, the above two solutions do not have robustness for image super resolution reconstruction.

Hypothesis e has the property of independent and identical distribution, let $f_\theta(e_i)$ be its probability density function and θ represent the adjustment parameters of probability distribution. If the sparsity of α is not considered, its likelihood function can be estimated as $L_\theta[e_1, e_2, \cdots, e_n]=\prod_{i=1}^{n} f_\theta(e_i)$. The maximum likelihood estimation criterion is the minimized objective function: $-\ln L_\theta=\sum_{i=1}^{n}\rho_\theta(e_i)$, where $\rho_\theta(e_i)=-\ln f_\theta(e_i)$. If we consider the sparseness of α, the problem of sparse coding can be expressed as (σ is a constant):

$$\min_{\alpha} \sum_{i=1}^{n}\rho_\theta(e_i) \text{ s.t. } \|\alpha\|_1 \leqslant \sigma \tag{6}$$

that is

$$\min_{\alpha} \sum_{i=1}^{n}\rho_\theta(y_i-p_i\alpha) \text{ s.t. } \|\alpha\|_1 \leqslant \sigma \tag{7}$$

The essence of the Ep.(7) is the maximum likelihood estimation problem with sparsity constraints, and can also be considered as a more general sparse coding problem, that is:

$$\min\|H(Y-D\alpha)\| \tag{8}$$

The Eq.(8) is called the weighted norm approximation [15], and H is the diagonal weight matrix. In order to ensure the accuracy of image reconstruction, different decomposed residuals should correspond to different weights. Yang et al.[16] gave the definition of H to solve the problem of sparse decomposition in face recognition. We defines H as follows:

$$H_{i,i}=\frac{\exp\left(Ae_i^2\right)g\left(\left|e_i^2\right|\right)}{\sum_{i=1}^{n}\exp\left(Ae_i^2\right)g\left(\left|e_i^2\right|\right)} \tag{9}$$

Where A represents the control constant, $g(\cdot)$ means a Gaussian function with a mean of 0 and a standard deviation of 3.

By the above analysis, Eq.(7) can be expressed by the least square solution that conforms to the mixed Gaussian distribution:

$$\hat{\alpha}=\min_{\alpha}\left|\left|H^{1/2}(Y-D\alpha)\right|\right|_2^2+\eta\|\alpha\|_1 \tag{10}$$

Where η is a constant. A solution of α can be obtained by the iterative contraction algorithm until the weight matrix converges.

1.3 Proposed model

Hyperspectral images have spectral properties, and all the bands of the same pixel constitute the one-dimensional spectral information of the pixel. Hyperspectral images have high spectral resolution and strong correlation between neighboring bands. Using spectral features can better classify targets. In order to better preserve the image spectral information, ensure the accuracy of the reconstructed image, inspired by literature[13], the spectral correlation of hyperspectral image, we added the spectral correlation of hyperspectral images as a sparsely constrained condition to the super-resolution algorithm to improve the fidelity of the reconstructed image. The difference is that literature[13] uses the first L spectral information after the principal component analysis, and we use all the spectral information of the image. This is much more accurate, but it takes longer, so we have improved the algorithm to minimize running time. In addition, compared with literature[13], we construct a mixture Gaussian sparse coding model, which improves the spatial resolution of the reconstructed image and the robustness to noise.

Let $X(i, j, \lambda) \in R^{N_1\times N_2\times D}$ denote hyperspectral images, where $i=1, \cdots N_1$, $j=1, \cdots N_2$, $\lambda=1, \cdots D$, D denotes the number of bands in $X(i, j, \lambda)$, and $N=N_1\times N_2$ denotes the size of each image. $X_{i,j} \in R^D$ indicates the pixel spectrum at coordinate (i, j) in $X(i, j, \lambda)$, $X_\lambda \in R^N$ indicates the λ th band image in $X(i, j, \lambda)$, and $x(i, j, \lambda)$ indicates the pixel value at the coordinate (i, j) in the λ th band image. $\hat{X}(i, j, \lambda) \in R^{N_1\times N_2\times D}$

represents the reconstructed hyperspectral images, $\hat{X}_{i,j} \in R^D$ indicates the pixel spectrum at coordinate (i, j) in $\hat{X}(i, j, \lambda)$, $\hat{X}_\lambda \in R^N$ indicates the λ th band image in $\hat{X}(i, j, \lambda)$, and $\hat{x}(i, j, \lambda)$ indicates the pixel value at the coordinate (i, j) in the λ th band image.

First, the initial $\hat{X}(i, j, \lambda)$ is obtained by interpolation, and then, for each $\hat{X}_{i,j}$, the similar $\hat{X}_{i_k, j_k}$ is found in the reconstructed image, and the difference between them is calculated via:

$$\delta_{i,j}^k = \left\| \hat{X}_{i,j} - \hat{X}_{i_k, j_k} \right\|_2^2 \tag{11}$$

Take the first K $\hat{X}_{i_k, j_k}$ (k=1, …,K) that are most similar to $\hat{X}_{i,j}$ and $\hat{x}(i, j, \lambda)$ is denoted by $\hat{x}(i_k, j_k, \lambda)$ in $\hat{X}_{i_k, j_k}$, that is:

$$\hat{x}(i, j, \lambda) \approx \sum_{k=1}^K F_{i,j,\lambda}^k \hat{x}(i_k, j_k, \lambda) \tag{12}$$

In the formula,

$$F_{i,j,\lambda}^k = \frac{\exp\left(A' \delta_{i,j}^k\right) g\left(\left|\hat{x}(i, j, \lambda) - \hat{x}(i_k, j_k, \lambda)\right|\right)}{\sum_{k=1}^K \exp\left(A' \delta_{i,j}^k\right) g\left(\left|\hat{x}(i, j, \lambda) - \hat{x}(i_k, j_k, \lambda)\right|\right)}$$

Where A' represents the control constant, $g(\cdot)$ means a Gaussian function with a mean of 0 and a standard deviation of 3, that is:

$$\sum_{\hat{x}(i,j,\lambda) \in \hat{X}} \left\| \hat{x}(i, j, \lambda) - \sum_{k=1}^K F_{i,j,\lambda}^k \hat{x}(i_k, j_k, \lambda) \right\|_2^2 = \left\| \hat{X} - B\hat{X} \right\|_2^2 = \| (I - B) D\alpha \|_2^2 \tag{13}$$

in the form: I is the unit matrix, and the B is the weight matrix. The Eq.(13) is brought into the formula (10) as a sparse constraint condition, then:

$$\hat{\alpha} = \min_\alpha \left\{ \left\| H^{1/2}(Y - D\alpha) \right\|_2^2 + \eta \|\alpha\|_1 + \gamma \| (I - B) D\alpha \|_2^2 \right\} \tag{14}$$

η and γ represent the weight of the sparse constraint. Equation (14) is the sparse super-resolution mathematical model of hyperspectral images based on spectral correlation.

1.4 Proposed algorithm

Figure 1 is the basic idea of our algorithm. Firstly, the degraded model (Eq.(2)) is used to obtain the training samples $\{X, Y\}$(X is randomly selected in hyperspectral images), X and Y represent the high/low resolution image samples, and then the dictionary is learned by using the sparse coding Gaussian mixture model, and D_h and D_l are obtained according to the downsampling multiple. Secondly, the initial reconstruction image X_l is obtained by bicubic interpolation, and then the image blocks are taken one by one, and the sparse representation coefficients are obtained by sparse coding using the proposed super-

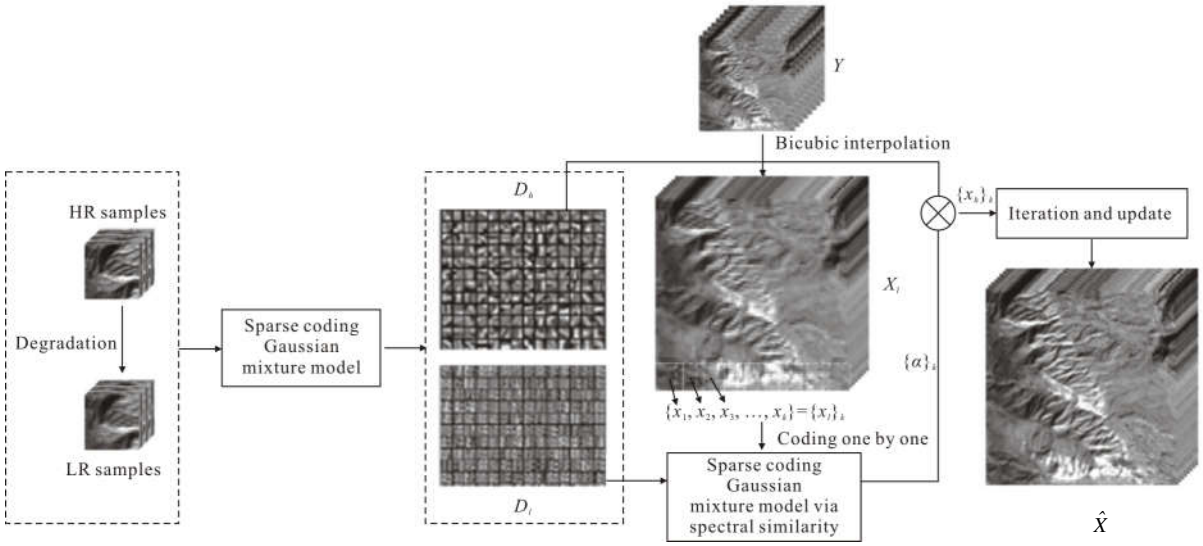

Fig.1 Basic idea of the proposed algorithm

resolution algorithm. Finally, reconstructed image $\hat{X}$ is obtained by using the method proposed by our research group[17].

Our algorithm is as follows:

Input	D_h, D_l, and $Y(i, j, \lambda)$;
Output	High resolution image $\hat{X}(i, j, \lambda)$;
Initialization	Total number of image blocks N, size of image block $n*n$, setting overlapped area;
Step 1	Initial reconstruction image $X_l(i, j, \lambda)$(obtained by interpolation of $Y(i, j, \lambda)$);
Step 2	According to the overlapped region, $n*n$ image blocks $\{x_l\}_k$ are obtained in order, and then each image block is subjected to sparse coding in D_l using Eq.(14) to obtain a set $\{\alpha\}_k$ and synchronously update B and H;
Step 3	The high-resolution image blocks $\{x_h\}_k$ are obtained by Eq.(3);
Step 4	The image blocks $\{x_h\}_k$ in each band are reconstructed, and $\hat{X}(i, j, \lambda)$ are obtained.

2 Experiment

2.1 Experimental environment and setting

A hyperspectral image from the outskirts of California is used in the experiment. The spectral coverage is 408.9-986.8 nm, the number of bands is 124, and the spectral resolution is 4 -5 nm. Our method compared the methods with Bicubic, Yang et al.[18] from the aspects of visual effects, general image evaluation index and hyperspectral image evaluation index to verify the effectiveness. Low resolution images are needed in the experiment based on the high resolution image in turn 2 times down sampling, mixed Gauss noise generated. In the experiment, the image block size is set to 5×5, the number of image blocks are 100 000, the dictionary size is 512, the overlapped region is 3, K=10, η=0.15, and γ=0.14. Experimental environment: Matlab7.10.0 runs on the HP2080 (Dual-core 2.8 GHz+2.0 G RAM) Windows XP SP3 platform.

2.2 Results and comparisons

Figure 2 (a) shows the 60th band hyperspectral image (200×300 in size), and Fig.2(b) shows the low resolution image obtained by down -sampling and adding mixed Gaussian noise (average noise variance 0.000 2 and 100×150 in size).

Figure 3 is a partial images of the 25th, 50th, 75th, and 100th band images that are reconstructed

(a) Original image(HR image)

(b) LR image

Fig.2 60th band hyperspectral image and processed low-resolution image

using different super -resolution algorithms (Bicubic, Yang, Pan, and our algorithm). From the visual effect of reconstruction. The results from Bicubic algorithm make the edge contour of the image blur, and the sawtooth effect is more obvious, such as the roof in the 25th and 75th band images; the results from Yang and Pan algorithm can better maintain the outline of the image, and many small -scale details are more clear, but the local denoising effect is not ideal, such as vegetation and road in the 50th and 100th band images; our results further improve the contour and local details, and has a significant effect on noise suppression.

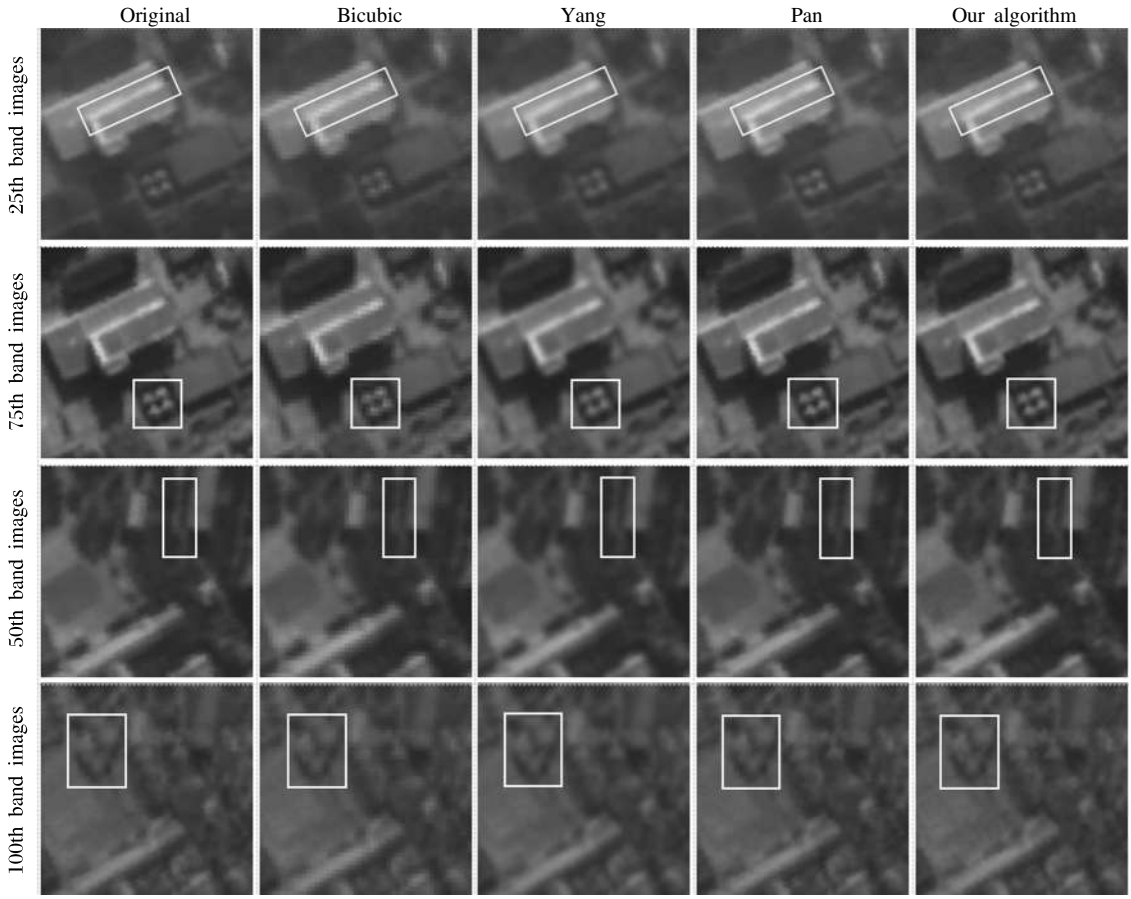

Fig.3 Results of super-resolution reconstruction of 25th, 75th, 50th and 100th band images

In order to objectively evaluate the reconstruction effect of each algorithm, we adopts PSNR and SSIM (full reference image quality assessment methods) and BRISQUE[19] (a no reference image quality assessment method) to evaluate the super-resolution reconstruction of single-band image.

BRISQUE algorithm believes that the image normalized luminance value tends to a normal Gaussian distribution, image distortion will change the statistical properties of the normalization coefficient, and the image is evaluated by measuring this characteristic. The smaller the BRISQUE value, the better the reconstruction effect.

Figure 4 compares the results of the three image evaluation methods under different algorithms. Table 1 is the PSNR value, SSIM value and BRISQUE value of the 25th and 100th band images under different algorithms, where the bold value corresponds to the optimal algorithm. Experimental data show that compared with Bicubic, Yang and Pan′s algorithm, our algorithm achieves better results.

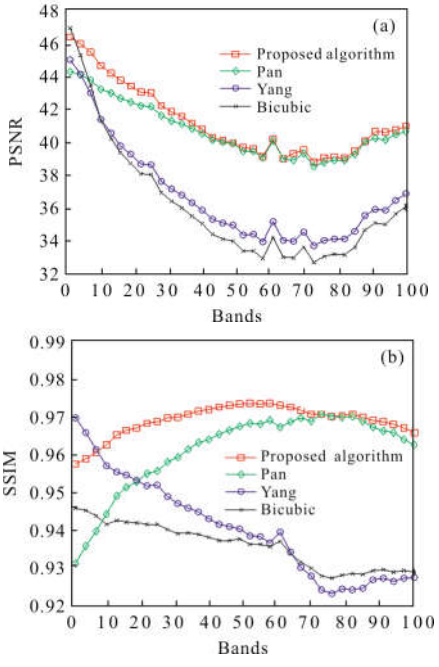

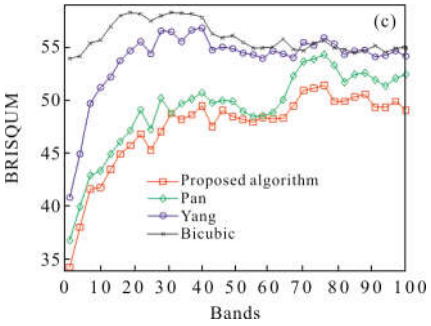

Fig.4 Comparison of the results of three image evaluation methods under different algorithms

Tab.1 Comparison of PSNR value, SSIM value and BRISQUE value of images under different algorithms

		PSNR	SSIM	BRISQUE
25th band	Bicubic	38.06	0.941 5	57.48
	Yang	38.65	0.951 8	54.38
	Pan	42.19	0.955 6	47.25
	Proposed algorithm	**43.03**	**0.968 6**	**45.29**
100th band	Bicubic	36.10	0.928 6	54.97
	Yang	36.87	0.927 2	54.17
	Pan	40.67	0.962 3	52.41
	Proposed algorithm	**40.99**	**0.965 7**	**49.04**

In addition, we also used the evaluation method of hyperspectral image to measure the super-resolution results[20], which are the average of PSNR, SSIM and SPSIM (APSNR, ASSIM, and ASPSIM).

$$APSNR=10\lg\left(\frac{\frac{1}{D}\sum_{\lambda=1}^{D}M_{\lambda}^{2}}{MSE}\right) \tag{15}$$

Where M_{λ} is the peak of X_{λ}.

$$ASSIM=\frac{1}{D}\sum_{\lambda=1}^{D}S_{\lambda} \tag{16}$$

Where S_{λ} (λ=1, $\cdots$,D) is the value of SSIM of the λth band image.

$$ASPSIM=\frac{1}{MN}\sum_{i=1}^{M}\sum_{j=1}^{N}R_{ij} \tag{17}$$

Where R_{ij} is the correlation coefficient of the original and the reconstructed image pixel spectrum, that is:

$$R_{ij}=\frac{\sum_{\lambda=1}^{D}\left[x(i,j,\lambda)-x_{i,j}\right]\left[\hat{x}(i,j,\lambda)-\hat{x}_{i,j}\right]}{\sqrt{\sum_{\lambda=1}^{D}\left[x(i,j,\lambda)-x_{i,j}\right]^{2}}\sqrt{\sum_{\lambda=1}^{D}\left[\hat{x}(i,j,\lambda)-\hat{x}_{i,j}\right]^{2}}} \tag{18}$$

Where $x_{i,j}$ is the mean of $X_{i,j}$ and $\hat{x}_{i,j}$ is the mean of $\hat{X}_{i,j}$. The greater the value of *APSNR* and *ASSIM*, the higher the spatial resolution of the reconstructed image, and the greater the value of *ASPSIM*, the more accurate the pixel spectrum of the reconstructed image is.

Table 2 compares the results of three evaluation indexes and calculation time under different algorithms. The experimental results show that the computational time of our algorithm is basically the same as that of the Pan′s, and the reconstruction effect is the best among the four algorithms, which not only improves the spatial resolution effectively, but also improves the accuracy of the pixel spectrum.

Tab.2 Comparison of the results of three evaluation indexes and calculation time under different algorithms

	APSNR	ASSIM	ASPSIM	Time/s
Bicubic	36.14	0.935 8	0.935 0	12.93
Yang	36.79	0.940 2	0.992 1	2 115.10
Pan	40.75	0.958 1	0.993 2	**955.66**
Proposed algorithm	**41.25**	**0.969 1**	**0.995 4**	982.08

Figure 5 is the comparison of the values of APSNR, ASSIM and ASPSIM under different noise intensity. The input image is divided into multiple image blocks, and the different image blocks are added to the different intensity of Gaussian mixture

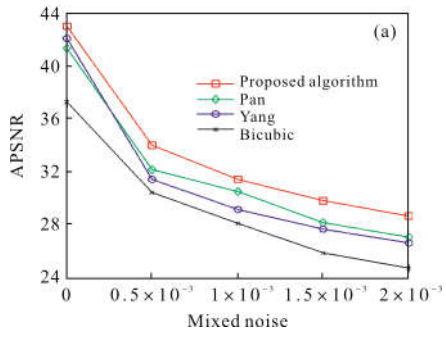

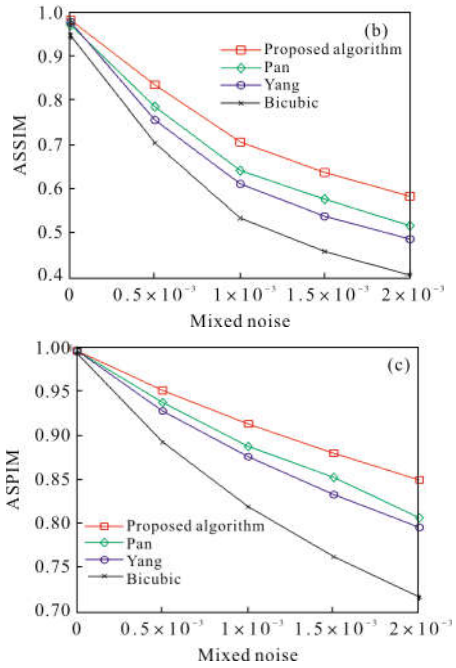

Fig.5 Comparison of the results under different noise intensity

noise and then merged before reconstruction. The results show that our algorithm is better than the others, which shows that our algorithm is robust to the Gaussian mixture noise.

2.3 Parameter analysis

The effects of the parameters on the reconstruction (no noise in the following experiments) have been analyzed as below.

2.3.1 Dictionary and sample size

To ensure better reconstruction of image structure and texture, the training dictionary should contain as many structural types as possible, and the number of samples should be enough. However, in actual application scenario, more training data will result in longer model training time.

Figure 6 compares the results of 60th band image when the dictionary size is 256, 512, and 1 024 respectively (the other parameters are the same). The value of PSNR is 39.07, 39.20 and 39.14 dB respectively, and the value of SSIM is 0.977 5, 0.978 3 and 0.978 0, respectively. The data show that the effect of reconstruction has no obvious change with the increase of the dictionary size in a certain range. Therefore, in the premise of ensuring the effect of reconstruction, a dictionary of suitable size can be used to shorten the time of dictionary training and image reconstruction as much as possible.

Fig.6 Comparison of the results of 60th band image under different dictionary size

Figure 7 compares the values of APSNR, ASSIM, and ASPSIM for reconstructed samples with different sample sizes. The sample size is between 20 000 and 140 000. From the figure, it can be seen that the effect changes little when the number of samples is different, and the effect is optimal when the number of samples is 80 000 to 100 000. This is because the number of samples is too small to provide a wealth of information such as image structure and texture, and

when the number of samples is too large, structures and textures may be inaccurately selected and time-consuming.

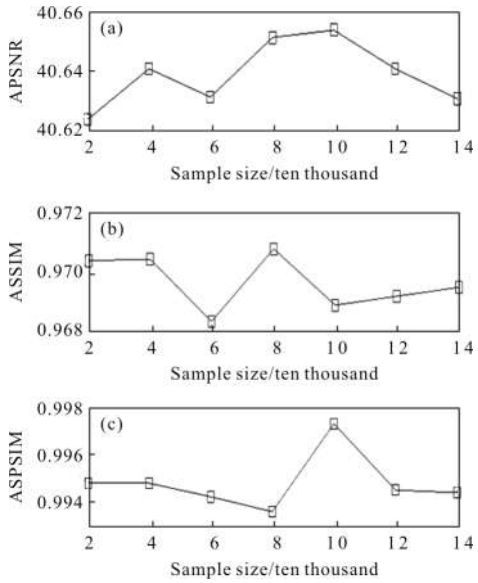

Fig.7 Comparison of the results under different sample size

2.3.2 Image block and overlapped region size

The image block in reconstruction is too small to produce distortion, which makes the image quality worse, and the detail information of images will be lost when the block is too large, which will result in the loss of . Figure 8 shows that the reconstruction effect is best when the size of the image block is 5×5. Figure 9 and Fig.10(the size of the image block is 7×7) show that the reconstruction effect is close to the best when the overlap area is around the 1/2 of the image block size.

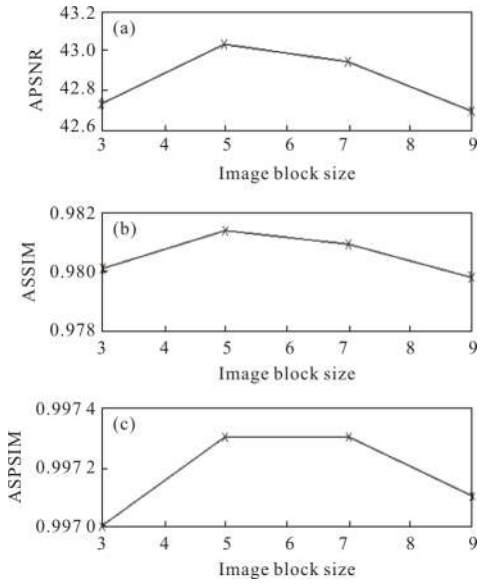

Fig.8 Comparison of the results under different image block size

Figure 9 is the local result of the reconstruction of the seventieth band images when the other parameters are the same, and the overlapped regions are 2, 4, and 6 respectively. Figure 10 is a comparison of the results of reconstruction under different overlapped regions. The overlap area is 2-6 (the size of the image block is 7×7). It is known from the graph that the more overlapping areas, the longer the time used for reconstruction, so 4 of the overlapped area is appropriate.

Fig.9 Comparison of the results of 70th band image under different overlapped region

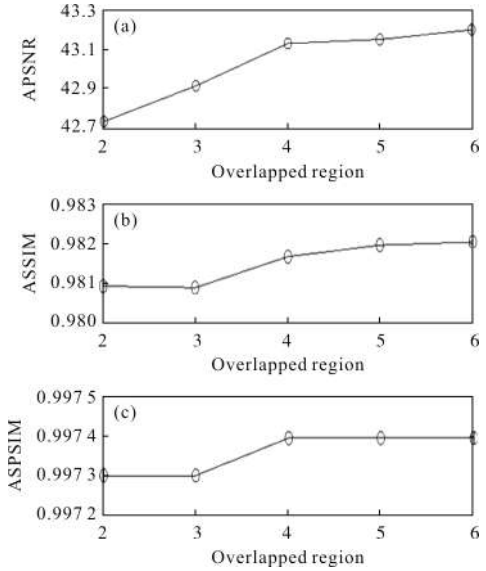

Fig.10 Comparison of the results under different overlapped region

2.3.3 Spectral constraint coefficient

Figure 11 shows that the result is best when γ= 0.14.

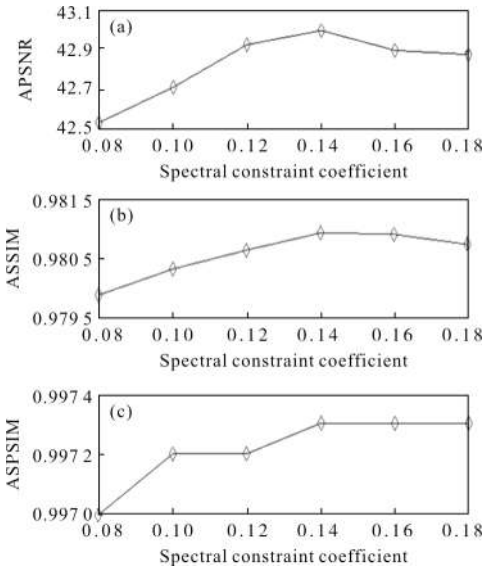

Fig.11 Comparison of the results under different spectral constraint coefficient

2.3.4 Super-resolution rate

Figure 12 shows that the reconstruction effect of all algorithms decreases with the increase of the super-resolution rate, but our algorithm is always optimal.

Based on the above analysis, we choose that the dictionary size is 512, the sample size is 100 000, image block size is 5×5, the overlapped region is 3, γ=0.14, and the super-resolution rate is 2.

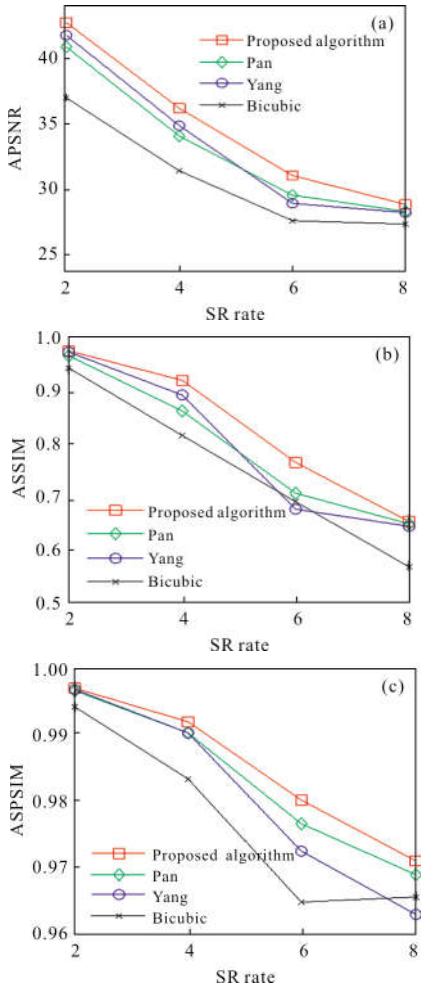

Fig.12 Comparison of the results under different super-resolution rate

3 Conclusion

A hyperspectral image super-resolution algorithm via sparse representation based on spectral similarity is proposed. Firstly, a sparse coding Gaussian mixture model is constructed under the criterion of maximum likelihood estimation. In this model, different weights are assigned according to the size of the decomposition residuals to enhance the effect of the reconstructed image and the robustness to noises. Secondly, the spectral similarity is used as a sparse constraint to construct a super-resolution model to improve the spectral fidelity. Finally, the parameters of the algorithm are analyzed in detail and the results show that both subjective and objective indicators of

our algorithm outperformed Bicubic, Yang and Pan′s algorithm, with the effectiveness being verified.

References:

[1] Tang Yi, Wan Jianwei, Nian Yongjian. Distributed near lossless compression of hyperspectral images[J]. ***Acta Optica Sinica***, 2015, 35(3): 0310001.

[2] Juefei-Xu F, Savvides M. Single face image super-resolution via solo dictionary learning[C]//IEEE International Conference on Image Processing (ICIP), 2015: 2239-2243.

[3] Wang Yiqun, Yan Changxiang, Miao Chun′an. Choice of spectral-splitting modes in space-borne hyperspectral imager [J]. ***Chinese Journal of Optics and Applied Optics***, 2009, 2(4): 304-308. (in Chinese)

[4] Xiao J, Pang G, Zhang Y, et al. Adaptive shock filter for image super-resolution and enhancement [J]. ***Journal of Visual Communication and Image Representation***, 2016, 40: 168-177.

[5] Zhang K, Tao D, Gao X, et al. Learning multiple linear mappings for efficient single image super-resolution [J]. ***IEEE Transactions on Image Processing***, 2015, 24(3): 846-861.

[6] Harris J L. Diffraction and resolving power [J]. ***Journal of the Optical Society of America***, 1964, 54(7): 931-936.

[7] Goodman J W. Introduction to Fourier Optics [M]. New York: Mc Graw-Hill, 1968.

[8] Batz M, Eichenseer A, Selier J, et al. Hybrid super-resolution combining example-based single-image and interpolation-based multi-image reconstruction approaches[C]// 2015 IEEE International Conference on Image Processing (ICIP), 2015: 58-62.

[9] Zhou Jinghong, Zhou Cui, Zhu Jianjun, et al. A method of super-resolution reconstruction for remote sensing image based on non-subsampled contourlet transform [J]. ***Acta Optica Sinica***, 2015, 35(1): 0110001. (in Chinese)

[10] Lian Qiusheng, Zhang Wei. Image super-resolution algorithms based on sparse representation of classified image patches[J]. ***Acta Electronica Sinica***, 2012, 40(5): 920-925. (in Chinese)

[11] Zhao Y Q, Yang J X, Zhang Q Y, et al. Hyperspectral imagery super-resolution by sparse representation and spectral regularization[J]. ***EURASIP Journal on Advances in Signal Processing***, 2011, 2011(1): 87.

[12] Pan Zongxu, Yu Jing, Xiao Chuangbai, et al. Spectral similarity-based super resolution for hyperspectral images[J]. ***Acta Automatica Sinica***, 2014, 40(12): 2797-2807. (in Chinese)

[13] Fu Fazuo. Hyperspectral image super-resolution based on non-negative dictionary learning [D]. Xi′an: Xidian University, 2018. (in Chinese)

[14] Tropp J A, Wright S J. Computational methods for sparse solution of linear inverse problems [J]. ***Proceedings of the IEEE***, 2010, 98(6): 948-958.

[15] Boyd S, Van den berghe L. Convex Optimization [M]. Cambridge: Cambridge University Press, 2009: 291-293.

[16] Yang M, Zhang L, Yang J, et al. Robust sparse coding for face recognition [C]//IEEE Conference on Computer Vision and Pattern Recognition(CVPR), 2011: 625-632.

[17] Xu Guoming, Xue Mogen, Yuan Guangling. Image super-resolution reconstruction method via mixture gaussian sparse coding[J]. ***Opto-Electronic Engineering***, 2013, 40(3): 94-101. (in Chinese)

[18] Yang J C, Wright J, Huang T, et al. Image super-resolution via sparse representation [J]. ***IEEE Transactions on Image Processing***, 2010, 19(11): 2861-2873.

[19] Saad M A, Bovik A C, Charrier C. Model-based blind image quality assessment: a natural scene statistics approach in the DCT domain [J]. ***IEEE Transactions on Image Processing***, 2012, 21(8): 3339-9952.

[20] Akgun T, Altunbasak Y, Mersereau R M. Super-resolution reconstruction of hyperspectral images[J]. ***IEEE Transactions on Image Processing***, 2005, 14(11): 1860-1875.